Published in final edited form as:
J Am Chem Soc. 2009 May 13; 131(18): 6386–6388. doi:10.1021/ja9006723.

Mössbauer, NMR, Geometric, and Electronic Properties in S = 3/2 Iron Porphyrins

Yan Ling and **Yong Zhang***
Departments of Chemistry and Biochemistry, University of Southern Mississippi, 118 College Drive #5043, Hattiesburg, MS 39406, USA

Iron porphyrins with the intermediate spin S = 3/2 or admixed with S = 5/2 and 1/2 are models for a number of heme protein systems,[1,2] including cytochromes c'. They have been intensely investigated experimentally.[1-17] In particular, the ^{57}Fe Mössbauer quadrupole splittings and ^{1}H and ^{13}C NMR chemical shifts were found to be useful probes for their electronic states. However, specific relationships between these spectroscopic properties and geometric parameters have not been reported. There are also no reports of quantum chemical calculations of these important spectroscopic probes in S = 3/2 iron porphyrins, except for our recent work on the Mössbauer properties of one of such complexes.[18] In addition, their electronic states are under debate. While the early work suggested an electronic configuration of $(d_{xy})^2(d_{xz},d_{yz})^2(d_{z2})^1(d_{x2-y2})^0$ for S = 3/2 ferric porphyrins,[1] the more recent experimental work[4] discovered two possibilities, with this early proposed electronic state for saddled iron porphyrins and a new electronic configuration of $(d_{xz},d_{yz})^3(d_{xy})^1(d_{z2})^1(d_{x2-y2})^0$ for ruffled ones. However, a recent theoretical study proposed an opposite assignment of these two electronic states.[19]

Here, we present the results of the first quantum chemical calculations of the Mössbauer and NMR properties in various S = 3/2 iron porphyrins and their interesting new correlations with geometric and electronic properties. As shown in Table 1, the S = 3/2 complexes investigated here cover all possible coordination states of iron porphyrins: four, five, and six, as well as the commonly seen porphyrin conformations: planar, ruffled, and saddled.[3-5,7,9-14,16,17] In addition to almost pure S = 3/2 complexes (**1**, **3**, **4**, **5**), the one containing 20% S = 5/2 state (**2**) as well as the one related to those having spin crossover with S = 1/2 (**6**) were studied. A couple of spin admixed complexes with mostly S = 5/2 features (**7**, **8**) were also calculated for comparison. Experimental x-ray structures were used in all calculations using the DFT method that previously gave accurate predictions of Mössbauer quadrupole splittings (ΔE_Q) and isomer shifts (δ_{Fe})[18,20] and NMR ^{1}H and ^{13}C hyperfine shifts[21] for metalloproteins and models.[22]

Clearly, as seen from Table 1, the computational results support experimental findings that the Mössbauer quadrupole splittings and ^{1}H and ^{13}C NMR hyperfine shifts are sensitive probes of the spin states (S = 3/2 vs. 5/2 or 1/2), since for each of these complexes, only the calculated results from using the correct spin state for the x-ray structure are in good agreement with experimental spectroscopic data. As illustrated in Figure 1A, calculations of the experimental ΔE_Q results[3,10,12-14,17] have a theory-versus-experiment correlation coefficient $R^2 = 0.99$ and a standard deviation of 0.12 mm/s or 2.9% of the whole experimental range from 0.95 mm/s to 5.16 mm/s. These results extend previous computational work on iron-containing proteins

E-mail: yong.zhang@usm.edu.

Supporting Information Available: Computational details and other experimental information (Tables S1-S2 and Figures S1-S4) are available free of charge via the Internet at http://pubs.acs.org.

and models[18,20] to a total experimental range of 8.80 mm/s with R^2 = 0.98, Figure S1. The experimental Mössbauer isomer shifts were also well reproduced, Table 1. However, these data are insensitive to spin states and they only display a small range (see Figure 1B), which precludes its use as sensitive probes for these complexes. The ^{1}H NMR chemical shifts of pyrrole protons have long been recognized as good indicators of spin states in spin admixed 3/2, 5/2 complexes,[3,12,13,15] due to different spin density distributions between the intermediate and high spin states, which will affect the observed NMR hyperfine shift ($\delta_{hf}^{H\beta}$), a major component of the NMR chemical shift that is proportional to spin densities.[21,22] For porphyrins with substituents on the pyrrole proton positions, such as OEP and OETPP, the experimental NMR hyperfine shifts of the $-CH_2$ group of the ethyl substituents[4,7,9,10] ($\delta_{hf}^{HC\alpha}$) were also investigated. As shown in Table 1 and Figure 1C, the experimental ^{1}H NMR hyperfine shifts covering a range of 122.7 ppm were accurately predicted with R^2 = 0.99. The predicted ^{13}C NMR hyperfine shifts for porphyrin α-, β-, and meso-carbons ($\delta_{hf}^{C\alpha}$, $\delta_{hf}^{C\beta}$, δ_{hf}^{Cm}) are also in good agreement with experiment. Overall, the NMR predictions for these S = 3/2 systems are in the same trend line of previous calculations of proteins and models with other spin states,[21] Figure S2. These results provide a solid basis for using DFT calculations in investigating S = 3/2 ferric porphyrin systems.

Since these results represent the first successful calculations of experimental Mössbauer and NMR properties for a good variety of S = 3/2 iron porphyrins, we next investigated the relationships between these sensitive experimental probes and the structural features. Interestingly, the Mössbauer quadrupole splittings in these porphyrins (**1-8**) were found for the first time to have good correlations with the average bond lengths of iron and pyrrole nitrogen bonds, R_{FeN}. Although most complexes studied here have intermediate spins and only two are high spin species, this correlation can be extended to other high spin iron porphyrins and heme protein[18] (**9-12**, Table S2) as well. As depicted in Figure 1D, large quadrupole splittings are correlated with smaller Fe-N bond lengths with R^2 = 0.93 and this correlation is independent of coordination states and porphyrin conformations. It should be noted that the Mössbauer quadrupole splittings are also correlated well with other useful experimental spectroscopic properties, such as pyrrole proton NMR shifts and the magnetic susceptibilities.[15] Therefore, the quantitative relationship with Fe-N bond lengths may help structural investigations of the S = 3/2 and 5/2 heme proteins using a number of experimental techniques.

It is also interesting to note that among the S = 3/2 ferric porphyrins investigated here with three porphyrin coordination states (four, five, six) and three common porphyrin conformations (planar, ruffled, saddled), there are only two general trends of the porphyrin ^{13}C NMR hyperfine shifts based on both experimental and computational results and the trends were found to depend on the porphyrin conformation, not the coordination state: $\delta_{hf}^{C\alpha} < \delta_{hf}^{C\beta} < \delta_{hf}^{Cm}$ for planar and ruffled complexes, and the opposite trend of $\delta_{hf}^{C\alpha} > \delta_{hf}^{C\beta} > \delta_{hf}^{Cm}$ for saddled ones (see Table 1). This indicates an important effect of the porphyrin conformation on the electronic structures as discussed below. Previous work[4,8,19] suggests that the relative ordering of $d_{xz/yz}$ (or d_π) vs. d_{xy} can affect the ^{13}C NMR hyperfine shift trends in the ruffled and saddled S = 3/2 iron porphyrins. Unfortunately, controversial results were obtained in the past.[4,8,19] To resolve this problem and understand the above new observations of the ^{13}C NMR hyperfine shift trends in these intermediate spin ferric complexes with more varieties of porphyrin structures, we investigated all of the wavefunctions from above successful calculations. As shown in Figures 2A, 2E, 2I, 2M, S3A, and S4A, a common outcome of all these S = 3/2 complexes is that d_{x2-y2} is of the highest energy, supporting previous work.[1,4,8,19] However, as a result of the current comprehensive investigation, more possibilities of frontier MO orderings were discovered than before:

1) $d_{x2-y2} > d_\pi > d_{xy} > d_{z2}$ for complexes **1**, **3**, and **4**, see Figures 2A-D, S3A-D, S4A-D, respectively

2) $d_{x2-y2} > d_{z2} > d_{\pi} > d_{xy}$ for complex **2**, see Figure 2E-H

3) $d_{x2-y2} > d_{xy} > d_{\pi} > d_{z2}$ for complex **5**, see Figure 2I-L

4) $d_{x2-y2} > d_{xy} > d_{z2} > d_{\pi}$ for complex **6**, see Figure 2M-P

Based on these results, it seems that the MO ordering does not depend on the coordination state. In contrast, the porphyrin conformation was found to play an important role as shown in Figures 2 and S3-4. This is consistent with the above observations of the ^{13}C NMR results. Of particular interest is that, though altogether a number of different frontier MO orderings were discovered here, there are only two orderings concerning the iron d_{π} and d_{xy} orbitals:, $d_{\pi} > d_{xy}$ in planar and ruffled complexes and the opposite trend of $d_{\pi} < d_{xy}$ in the saddled ones, Figure 2. This kind of porphyrin conformation dependence is again the same as with the porphyrin ^{13}C NMR hyperfine shifts, suggesting that the porphyrin conformation affects the relative ordering of d_{π} and d_{xy} orbitals, which are responsible for the observed porphyrin ^{13}C NMR results. This is because among the three types of occupied iron d orbitals (d_{π}, d_{xy}, d_{z2}), only d_{π} and d_{xy} orbitals have significant contributions to the spin densities in the porphyrin ring, while the d_{z2} orbital mainly influences axial ligands. Another interesting new observation is that the d_{z2} ordering depends on the Fe-N distance. As shown in Figures 2 and S3-4, among the planar and ruffled S = 3/2 complexes, d_{z2} is usually of the lowest energy when R_{FeN} is small, due to the weaker interaction along the z-axis compared to the stronger ones in the x-y plane from shorter Fe-N contacts. However, when R_{FeN} is long ($\geq$ 1.975 Å), d_{z2} is higher than d_{π} as usual. The same kind of dependence of d_{z2} on R_{FeN} was also found with the saddled S = 3/2 porphyrins, see Figure 2.

Overall, the results presented above should facilitate future investigations of related iron porphyrins and heme proteins.

Supplementary Material

Refer to Web version on PubMed Central for supplementary material.

Acknowledgment

This work was supported in part by the NSF EPSCoR award OIA-0556308 and NIH grant GM-085774.

References

1. Weiss R, Gold A, Terner J. Chem. Rev 2006;106:2550–2579. [PubMed: 16771459]
2. Zeng YH, Caignan GA, Bunce RA, Rodriguez JC, Wilks A, Rivera M. J. Am. Chem. Soc 2005;127:9794–9807. [PubMed: 15998084]
3. Fang M, Wilson SR, Suslick KS. J. Am. Chem. Soc 2008;130:1134–1135. [PubMed: 18171069]
4. Nakamura M. Coord. Chem. Rev 2006;250:2271–2294.
5. Hoshino A, Ohgo Y, Nakamura M. Inorg. Chem 2005;44:7333–7344. [PubMed: 16212360]
6. Yatsunyk LA, Shokhirev NV, Walker FA. Inorg. Chem 2005;44:2848–2866. [PubMed: 15819574]
7. Yatsunyk LA, Walker FA. Inorg. Chem 2004;43:757–777. [PubMed: 14731040]
8. Sakai T, Ohgo Y, Ikeue T, Takahashi M, Takeda M, Nakamura M. J. Am. Chem. Soc 2003;125:13028–13029. [PubMed: 14570467]
9. Ikeue T, Ohgo Y, Ongayi O, Vicente MGH, Nakamura M. Inorg. Chem 2003;42:5560–5571. [PubMed: 12950204]
10. Ikeue T, Ohgo Y, Yamaguchi T, Takahashi M, Takeda M, Nakamura M. Angew. Chem. Int. Ed 2001;40:2617–2620.
11. Barkigia KM, Renner MW, Fajer J. J. Porphyr. Phthalocyanines 2001;5:415–418.

12. Ikeue T, Saitoh T, Yamaguchi T, Ohgo Y, Nakamura M, Takahashi M, Takeda M. Chem. Commun 2000:1989–1990.

13. Simonato JP, Pecaut J, Le Pape L, Oddou JL, Jeandey C, Shang M, Scheidt WR, Wojaczynski J, Wolowiec S, Latos-Grazynski L, Marchon JC. Inorg. Chem 2000;39:3978–3987. [PubMed: 11198850]

14. Schunemann V, Gerdan M, Trautwein AX, Haoudi N, Mandon D, Fischer J, Weiss R, Tabard A, Guilard R. Angew. Chem. Int. Ed 1999;38:3181–3183.

15. Reed CA, Guiset F. J. Am. Chem. Soc 1996;118:3281–3282.

16. Scheidt WR, Geiger DK, Lee YJ, Reed CA, Lang G. Inorg. Chem 1987;26:1039–1045.

17. Debrunner, PG. Iron Porphyrins. Lever, ABP.; Gray, HB., editors. Vol. 3. VCH Publishers; New York: 1989. p. 139-234.

18. a Zhang Y, Mao J, Oldfield E. J. Am. Chem. Soc 2002;124:7829–7839. [PubMed: 12083937] b Zhang Y, Mao J, Godbout N, Oldfield E. J. Am. Chem. Soc 2002;124:13921–13930. [PubMed: 12431124]

19. Cheng RJ, Wang YK, Chen PY, Han YP, Chang CC. Chem. Commun 2005:1312–1314.

20. a Zhang Y, Gossman W, Oldfield E. J. Am. Chem. Soc 2003;125:16387–16396. [PubMed: 14692781] b Zhang Y, Oldfield E. J. Phys. Chem. B 2003;107:7180–7188. c Zhang Y, Oldfield E. J. Phys. Chem. A 2003;107:4147–4150. d Zhang Y, Oldfield E. J. Am. Chem. Soc 2004;126:4470–4471. [PubMed: 15070336] e Zhang Y, Oldfield E. J. Am. Chem. Soc 2004;126:9494–9495. [PubMed: 15291525]

21. a Mao J, Zhang Y, Oldfield E. J. Am. Chem. Soc 2002;124:13911–13930. [PubMed: 12431123] b Zhang Y, Oldfield E. J. Am. Chem. Soc 2008;130:3814–3823. [PubMed: 18314973]

22. see Supporting Information for computational details.

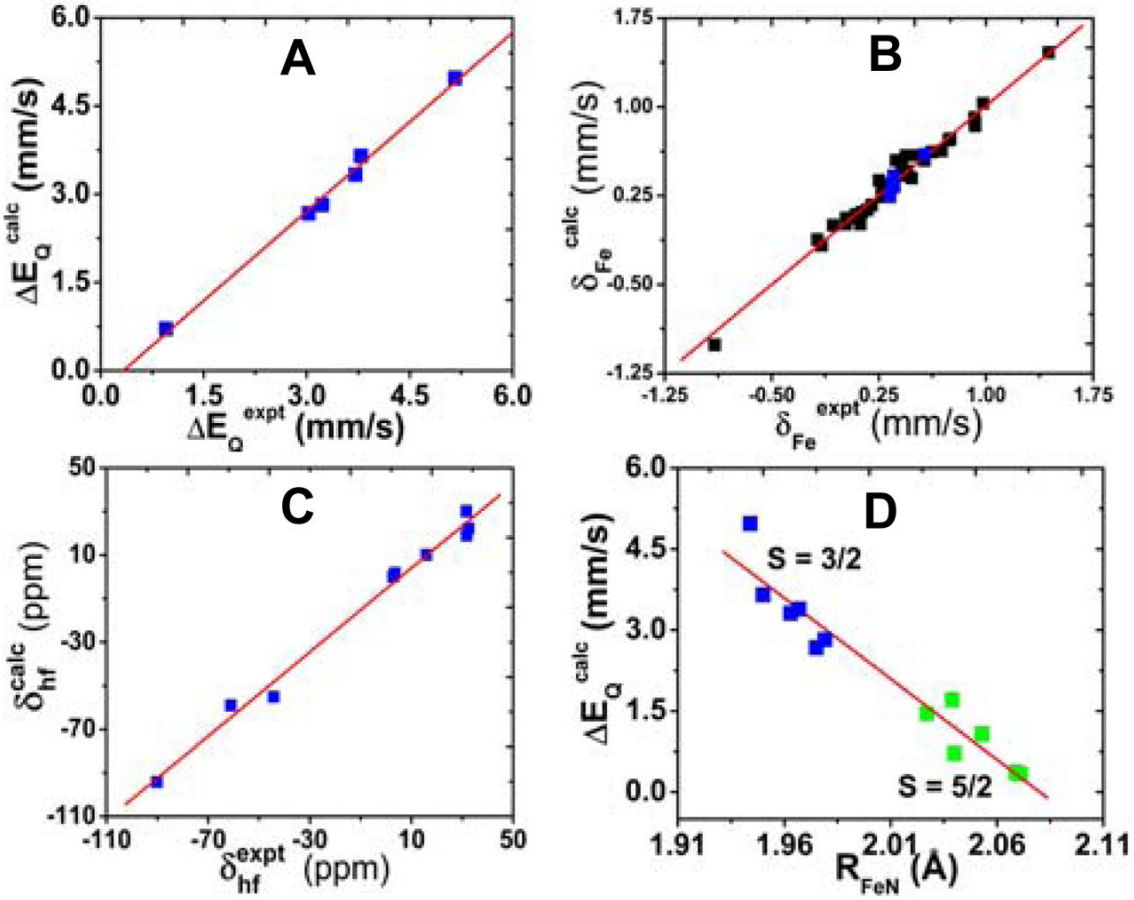

Figure 1.

A. Computed Mössbauer quadrupole splittings vs. experimental data. **B**. Calculated Mössbauer isomer shifts vs. experimental results. **C**. Calculated ^{1}H NMR hyperfine shifts vs. experimental data. **D**. Relationship between ΔE_Q and R_{FeN}. Blue and green data points are from this work and black data points are from previous work, refs 18 and 20.

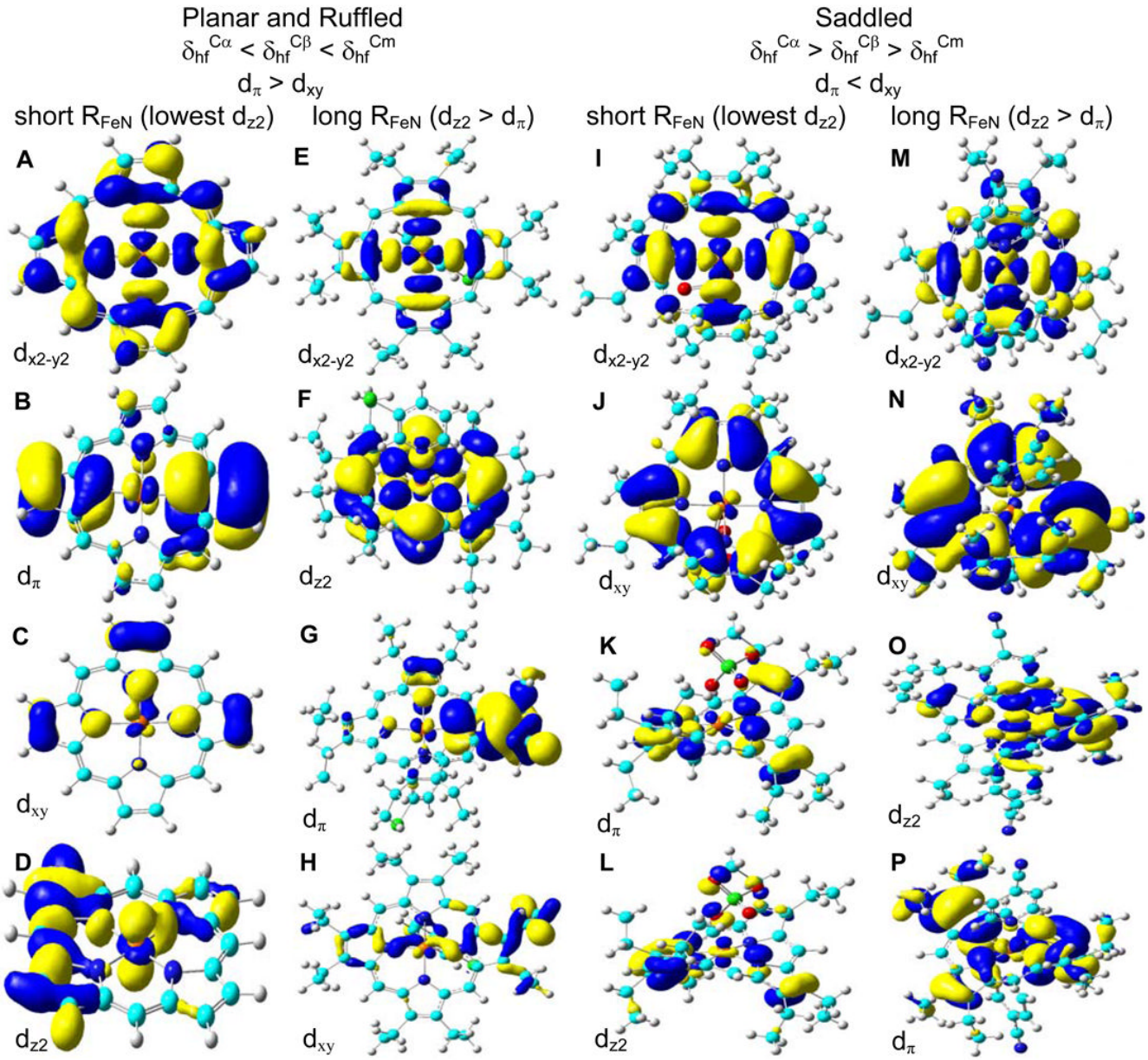

Figure 2.

Summary of the structural dependence for porphyrin ^{13}C NMR trends and MO orderings and the isosurface representations of α-LUMO (**A**), α-HOMO-2 (**B**), β-HOMO-3 (**C**), and α-HOMO-12 (**D**) for **1**, α-LUMO (**E**), α-HOMO-1 (**F**), α-HOMO-2 (**G**), and α-HOMO-12 (**H**) for **2**, α-LUMO+1 (**I**), β-HOMO (**J**), α-HOMO-2 (**K**), and α-HOMO-5 (**L**) for **5**, α-LUMO+2 (**M**), α-HOMO (**N**), α-HOMO-2 (**O**), and α-HOMO-3 (**P**) for **6**, with contour values = ± 0.02, 0.02, 0.04, 0.04, 0.02, 0.02, 0.02, 0.04, 0.02, 0.02, 0.04, 0.04, 0.02, 0.01, 0.02, and 0.02 au, respectively.

Table 1

Mössbauer, NMR, Geometric, and Electronic Properties in S = 3/2 and 5/2 Iron Porphyrins [a]

Complex		S	R_{FeN} (Å)	ΔE_Q (mm/s)	δ_{Fe} (mm/s)	$\delta_{hf}^{H\beta}$ (ppm)	$\delta_{hf}^{HC\alpha}$ (ppm)	$\delta_{hf}^{C\alpha}$ (ppm)	$\delta_{hf}^{C\beta}$ (ppm)	δ_{hf}^{Cm} (ppm)	Ref
1 [Fe(TipsiPP)]$CB_{11}H_6Br_6$	Expt	3/2	1.944	5.16	0.33	−90.2					3
4-coordinate	Calc	3/2		4.97	0.24	−94.2	/	−509.9	−195.1	−100.6	
Planar		5/2		4.10	0.27	−29.4	/	1795.1	1213.2	−350.5	
2 FeOEP(3-ClPy)	Expt	3/2	1.979	3.23	0.36						16’17
5-coordinate	Calc	3/2		2.82	0.33	/	26.7, 6.3	−470.2	−38.4	89.7	
Planar		5/2		1.98	0.34	/	56.3, 45.3	1304.6	1023.8	−46.8	
3 FeTMCP(H_2O)(EtOH)	Expt	3/2	1.950	3.79	0.35	−44.2					13
6-coordinate	Calc	3/2		3.65	0.32	−55.1	/	−313.7	−177.0	−28.4	
Ruffled		5/2		3.16	0.34	27.1	/	1418.5	1185.8	−31.8	
4 [Fe(T^iPrP)($THF)_2$]ClO_4	Expt	3/2	1.967	3.71	0.34	−61.1		−272.8	−110.5	−28.3	5’12
6-coordinate	Calc	3/2		3.33	0.35	−59.0	/	−299.7	−207.7	−44.4	
Ruffled		5/2		2.81	0.35	25.2	/	1588.4	1013.5	−92.0	
5 Fe(OETPP)ClO_4	Expt	3/2	1.963				32.5, 2.8				4’11
5-coordinate	Calc	3/2		3.31	0.40	/	22.2, 0.0	117.3	17.4	−120.5	
Saddled		5/2		3.27	0.40	/	205.5,25.7	1834.8	−371.7	−1854.5	
6 [FeOETPP(4-CNPy)$_2$]ClO_4	Expt	3/2	1.975	3.03	0.57		31.6, 3.5	318.8	133.1	−388.9	4’7’9’10
6-coordinate	Calc	3/2		2.67	0.60	/	30.1,1.6	201.3	11.1	−252.1	
Saddled		1/2		3.51	0.43	/	6.3,3.1	72.9	−50.8	158.5	
7 [Fe(TipsiPP)]CF_3SO_3	Expt	5/2	2.053								3
5-coordinate	Calc	5/2		1.07	0.46	59.3	/	1171.5	1140.6	178.7	
Planar		3/2		3.70	0.54	−10.4	/	−106.4	−226.5	60.6	
8 Fe(OETPP)Cl	Expt	5/2	2.040	0.95	0.35		31.7, 15.9				4’14
5-coordinate	Calc	5/2		0.71	0.42	/	19.0, 10.1	602.8	1004.6	314.2	
Saddled		3/2		1.88	0.48	/	3.1, 0.0	144.3	44.4	−87.2	

[a] TipsiPP = 5,10,15,20-tetrakis(2′,6′-bis(triisopropylsiloxy)phenylporphyrinato, OEP = 2,3,7,8,12,13,17,18-octaethylporphyrinato, TMCP = 5,10,15,20-tetramethylchiroporphyrinato, T^iPrP = 5,10,15,20-tetraisopropylporphyrinato, OETPP = 2,3,7,8,12,13,17,18-octaethyl-5,10,15,20-tetraphenylporphy-rinato. Temperatures of Mössbauer and NMR results are listed in Table S1.